HHS Public Access

Author manuscript

Toxicol Appl Pharmacol. Author manuscript; available in PMC 2020 January 01.

Published in final edited form as:

Toxicol Appl Pharmacol. 2019 January 01; 362: 9–19. doi:10.1016/j.taap.2018.09.026.

Effect of N-(2-Aminoethyl) Ethanolamine on Hypertrophic Scarring Changes *in Vitro*: Finding Novel Anti-Fibrotic Therapies

Zhenping Chen[1,2], **Jianhua Gu**[7], **Amina El Ayadi**[2,6], **Andres F. Oberhauser**[3,4], **Jia Zhou**[5], **Linda E. Sousse**[2,6], **Celeste C. Finnerty**[2,6], **David N. Herndon**[2,6], and **Paul J. Boor**[1,6,*]

[1]Department of Pathology, University of Texas Medical Branch, Galveston, TX 77555, USA.

[2]Department of Surgery, University of Texas Medical Branch, Galveston, TX 77555, USA.

[3]Department of Neuroscience and Cell Biology, University of Texas Medical Branch, Galveston, TX 77555, USA.

[4]Sealy Center for Structural Biology and Molecular Biophysics, University of Texas Medical Branch, Galveston, TX 77555, USA.

[5]Department of Pharmacology and Toxicology, University of Texas Medical Branch, Galveston, TX 77555, USA.

[6]Shriners Hospitals for Children, The Houston Methodist Hospital Research Institute, Galveston, TX 77550, USA.

[7]AFM/SEM Core Facility, The Houston Methodist Hospital Research Institute, Houston, TX 77030, USA.

Abstract

Hypertrophic scars (HS) limit movement, decrease quality of life, and remain a major impediment to rehabilitation from burns. However, no effective pharmacologic therapies for HS exist. Here we tested the *in vitro* anti-fibrotic effects of the novel chemical N-(2-aminoethyl) ethanolamine (AEEA) at non-toxic concentrations. Scanning electron microscopy showed that AEEA markedly altered the structure of the extracellular matrix (ECM) produced by primary dermal fibroblasts isolated from a HS of a burn patient (HTS). Compression atomic force microscopy revealed that AEEA stiffened the 3D nanostructure of ECM formed by HTS fibroblasts. Western blot analysis in three separate types of primary human dermal fibroblasts (including HTS) showed that AEEA exposure increased the extractability of type I collagen in a dose-and time-dependent fashion, while not increasing collagen synthesis. A comparison of the electrophoretic behavior of the same set of samples under native and denaturing conditions suggested that AEEA alters the 3D structure of type I collagen. The antagonization effect of AEEA to TGF-β1 on ECM formation was also observed. Furthermore, analyses of the anti-fibrotic effects of analogs of AEEA (with modified

*Corresponding author.

Conflict of interest

The authors state no conflict of interest.

pharmacophores) suggest the existence of a chemical structure–activity relationship. Thus, AEEA and its analogs may inhibit HS development; further study and optimization of analogs may be a promising strategy for the discovery for effective HS therapies.

Keywords

Atomic Force Microscopy (AFM); Collagen; Drug Discovery; Scanning Electron Microscopy (SEM); Wound Healing

Introduction

Hypertrophic scar (HS) is a thick, raised scar arising from exuberant, pathological growth of cutaneous tissue. HS is characterized by deposition of excessive amounts of collagen, which results in a bulky, inelastic, and raised mass (Scott et al., 2000; Bombaro et al., 2003; Gabriel, 2011; Butzelaar et al., 2016; Finnerty et al., 2016). HS is common after major burns and is a critical determinant of outcomes after cutaneous trauma. Up to 90% of severely burned patients have hypertrophic scarring (Deitch et al., 1983; Bombaro et al., 2003; Finnerty et al., 2016). HS restricts movement, causes many morbidities including pain, results in poor cosmesis, and greatly decreases quality of life (Gabriel, 2011; Tredget et al., 2014; Finnerty et al., 2016; Wurzer et al., 2017). Over the course of many decades, effective therapeutic strategies to counter HS formation have been sought. However, most therapeutic approaches remain clinically unsatisfactory, with the exception of surgical revision or laser treatment (Gauglitz et al., 2011). Because HS remains a major impediment to burn rehabilitation (Sheridan and Tompkins, 2004; Rhett et al., 2008; Gauglitz et al., 2011; Rabello et al., 2014), development of a therapeutic drug to attenuate or prevent HS development is a key goal in the long-term treatment of severe burns.

Abnormal and excessive ECM deposition during wound healing contributes to the formation of HS (Midwood et al., 2004; van der Veer et al., 2009; Reinke and Sorg, 2012; Carver and Goldsmith, 2013; Xue and Jackson, 2015). Type I collagen is the predominant mature collagen in most adult tissues, including mature normal scars and HS (Zgheib et al., 2014). During the fibrosis associated with normal wound healing, as well as in keloid and HS formation, the collagen content in the ECM (Zgheib et al., 2014) and the cross-linking of collagen (Moriguchi and Fujimoto, 1979; Uzawa et al., 1998; van den Bogaerdt et al., 2009) increases. Thus, hindering excess ECM accumulation by modifying the synthesis, assembly or cross-linking of collagen (Cohen, 1985) during the remodeling phase of wound healing, may reduce the formation of pathologic HS.

N-(2-aminoethyl) ethanolamine (AEEA, CAS RN 111–41-1), an aliphatic amine produced by chemical companies such as BASF (Baden Aniline and Soda Factory, Ludwigshafen, Germany) and Dow Chemical Company (Midland, Michigan, United States), has widespread use in industry as a chemical intermediate in the production of fabric softeners, chelating agents, surfactants, lubricating oil additives, fuel additives, hardeners, and soldering fluxes (Moore et al., 2012; Schneider et al., 2012b). AEEA induces aortic dissecting aneurysm in the offspring of rats exposed to the chemical during gestation (Moore et al., 2012; Schneider et al., 2012b). During studies of this developmental model of

dissecting aortic aneurysm in the rat, our laboratory found that AEEA markedly alters the development of the extracellular matrix (ECM) both *in vivo* and in isolated rat aortic vascular smooth muscle cells *in vitro* (Xu et al., 2014; Chen et al., 2015).

TGF-β1 is produced by immune cell lineages, including B, T, dendritic cells, macrophages (Moustakas et al., 2002), and activated fibroblasts during the formation of HS, and plays a key role in cutaneous wound healing and HS formation (Armour et al., 2007). TGF-β1 promotes recruitment of fibroblasts to the wound, encourages their proliferation, and induces fibroblasts to undergo a phenotypic change to myofibroblasts (Leask and Abraham, 2004). Thus, TGF-β1 stimulates synthesis of structural matrix proteins (e.g., collagen and fibronectin) (Piek et al., 2001), and remodeling of ECM (Roberts et al., 1986; Roberts et al., 1990; Nall et al., 1996; Blobe et al., 2000; Leask and Abraham, 2004; Xie et al., 2008; Penn et al., 2012; Zhang et al., 2012; Boo and Dagnino, 2013; Finnson et al., 2013; Hinz, 2015; Hinz, 2016). Nevertheless, efficient activation of latent TGF-β requires appropriate localization of latent complexes in the ECM (Taipale et al., 1996; Nunes et al., 1997; Annes et al., 2003; Dallas et al., 2005).

In this study, we investigated the potential *in vitro* anti-fibrotic effects of AEEA on ECM morphology using scanning electron microscopy (SEM), on biophysical property by atomic force microscopy (AFM) analysis, and on biochemical changes analyzed by Western blot. We also investigated the effects of AEEA on TGF-β1–mediated responses, which are thought to play a pivotal role in HS formation (Penn et al., 2012). Further, we tested several chemical analogs of AEEA and identified four with effects similar to those of AEAA, suggesting that a chemical structure–activity relationship (SAR) could be explored to develop novel HS therapies.

Materials and methods

Materials

AEEA was supplied by BASF SE, Ludwigshafen, Germany (lot number: AE4A0790H0; purity 99.8%). We purchased the following from Sigma-Aldrich (St. Louis, MO): the AEEA analogs diethylenetriamine (catalog # D93856), diethanolamine (catalog # D8885), 2-(2-(methylamino)-ethylamino)-ethanol (catalog # S522449), triethanolamine (catalog # 90279), 2-(2-aminoethoxy)ethanol (catalog # A54059), 2-(2-aminoethoxy)ethylamine (catalog # CDS000024); digitonin (catalog # 260746 Aldrich), sodium deoxycholate (catalog # D6750); (+)-sodium L-ascorbate (catalog # A4034); sodium phosphate dibasic (catalog # S0876); sodium phosphate mono basic (catalog # S0751); Trizma base (catalog # T-8524); Tween 20 (catalog # P9416); and urea (catalog # U5128), and chloramine T (catalog # 857319). Sodium chloride (catalog # 7581) was from Mallinckrodt Chemicals (Phillipsburg, NJ). Hydrochloric Acid (catalog # A144) and Ehrlich's solution (catalog # LC140802) were purchased from Fisher Scientific (Tampa, FL). Recombinant human TGF-β1 protein (catalog# GF111) was purchased from EMD Millipore. Protease inhibitor cocktail (cOmplete, EDTA-free Protease Inhibitor Cocktail Tablets, catalog # 05056489001) was from Roche Diagnostics (Indianapolis, IN). Novex NuPAGE SDS-PAGE gels (4-12% Bis-Tris pre-cast gels, catalog # NP0321), NuPAGE™ LDS sample buffer (4X) (catalog # NP0007), PageRuler™ plus prestained protein ladder (catalog # 26619), Invitrogen™

Novex™ 10X Bolt™ sample reducing agent (catalog # B0009), NuPAGE™ antioxidant (catalog # NP0005), NuPAGE MOPS SDS running buffer (catalog# NP0001), NuPAGE 7% Tris-Acetate native gel (catalog # EA0355), NativePAGE™ Novex™ 3-12% Bis-Tris protein gels (catalog # BN1001), Novex® Tris-Glycine native running buffer (catalog #LC2672), Novex® Tris-Glycine native sample buffer (2X) (catalog # LC2673) were obtained from Invitrogen Life Technologies Corporation, Thermo Fisher Scientific (Waltham, MA). Immobilon-P (PVDF) transfer membrane (catalog # IPVH00010) was from EMD Millipore (Billerica, MA). Antibody against type I collagen (catalog # ab34710) and secondary antibodies including anti-rabbit and anti-mouse IgG antibodies conjugated to horseradish peroxidase (catalog # ab6721 and ab6728, respectively) were from Abeam (Cambridge, MA). Antibody against GAPDH (catalog # sc-365062) was obtained from Santa Cruz Biotechnology, Inc. (Dallas, TX). Blue X-ray films (catalog # F-BX810) were from Phenix Research Products (Candler, NC), and Amersham ECL Western blotting detection reagent (catalog # RPN2106) was from GE Healthcare Bio-Sciences (Pittsburgh, PA). The MTT cell proliferation assay kit (catalog # ATCC® 30-1010K) was from American Type Culture Collection (Manassas, VA).

Human skin fibroblast culture and AEEA treatment

HTS fibroblasts utilized were primary dermal fibroblasts isolated from a HS of a burn patient, and NBS fibroblasts were isolated from non-burned skin; both cell lines were obtained from the same patient (Zhang et al., 2012). PCS are commercially available human primary dermal fibroblasts obtained from normal neonatal foreskin (catalog # ATCC® PCS-201-010™), and were purchased from American Type Culture Collection (Manassas, VA). Cells were cultured in Dulbecco's Modified Eagle’s Medium containing 4.5 g/L glucose, L-glutamine, and sodium pyruvate (catalog number 10-013-CV, Coming Life Sciences, Manassas, VA) and supplemented with 15% fetal calf serum (catalog # 10437028) and 1% 100 × Antibiotic-Antimycotic (catalog # 15240062) obtained from Gibco, Thermo Fisher Scientific (Waltham, MA). Cells were treated with AEEA as described previously (Chen et al., 2015). Sodium ascorbate (50 μg/ml), which is a crucial cofactor for lysyl oxidase, lysyl hydroxylase, and proline hydroxylase, was added daily for 5 days a week to stimulate ECM assembly (Pinnell, 1985; Pinnel et al., 1987; Davidson et al., 1997).

Cytotoxicity assays in dermal fibroblasts

The cytotoxicity of AEEA in the three primary human dermal fibroblast cell lines (HTS, NBS and PCS) was measured using a MTT cell proliferation assay kit, as described previously (He et al., 1998; Yang et al., 2004; Chen et al., 2015). The cells were incubated with varying concentrations of AEEA (0.0 to 40.0 mM). Absorbance was read at 570 nm with a microplate reader (FLUOStar Optima, BMG Lab tech, Cary, NC).

Preparation of decellularized matrix produced by human scar fibroblasts

The decellularized matrix samples were prepared using a previously described method (Chen et al., 2015). Briefly, cells were cultured as described above on 13-mm diameter coverslips (Nunc™ Thermanox™ coverslips, catalog #174950, Thermo Fisher Scientific, Waltham, MA) in 24-well cell culture plates. After AEEA treatments (0.0 to 100.0 μM), the resulting tissue sheets were gently rinsed twice with PBS and incubated in sterile deionized

water for 20 minutes at 4°C to lyse the cells under hypotonic conditions for decellularization. The water was then changed, and ECM samples were kept overnight at 4°C. The next day, the water was replaced with PBS. The ECM samples were used either for AFM without fixation or fixed for SEM with standard procedures (Chen et al., 2015).

Scanning electron microscopy

The SEM samples prepared on slides as described above were washed twice with PBS and processed as previously described (Chen et al., 2015). Specimens were scanned using a Nova NanoSEM 230 scanning electron microscope (FEI, Hillsboro, OR). All imaging (working distance of 5 mm, acceleration 5 to 8 kV) was performed at room temperature and under high vacuum (5E-6 Torr), and the images were obtained at a spot size of 2.5.

Atomic force microscopy

The mechanical properties of ECM samples were studied as described previously (Oberhauser et al., 1998; Chen et al., 2015). The rms force noise (1-kHz bandwidth) was ~10 pN. Unless noted, the compression and pulling speed of the different force–distance curves was in the range of 0.1 to 0.5 nm/ms. For estimation of Young's modulus using AFM, a controlled deformation was applied to the sample and the compressive forces were measured through the cantilever deflection (Fig. 3A). The force–displacement (F-x) curves were produced by converting cantilever deflection (d) into force (F) by means of $F = kd$, where k is the cantilever spring constant. The Young modulus (E) was estimated as described previously (Chen et al., 2015). To obtain accurate elasticity measurements in every sample, a $100 \times 100\ nm^2$ region was probed by running 100 force–displacement curves. The contact stiffness has the dimension of force per unit length and is calculated as the derivative of the upper ~30% of the unloading part of the compression curve. Agarose gel films served as a reference, since their Young's modulus is well known (Stolz et al., 2004; Loparic et al., 2010); the films were prepared using 2.5% (w/w) agarose (Sigma) in water as previously described (Stolz et al., 2004).

Protein detection via Western blot

Fibroblasts were cultured in 6-well plates (Corning™ Costar™, Catalog # 07-200-83) from Fisher Scientific (Tampa, FL), treated with varying concentrations of AEEA, and gently washed with 4°C pre-chilled PBS when harvested. Cross-linked collagens are not soluble; however, non-cross-linked collagens can be extracted depending on the strength of the extracting solution. Therefore, the samples were serially extracted, first with native lysis buffer containing 50 mM Tris-HCl (pH 7.5), 150 mM NaCl, and 1% digitonin (Demoliou-Mason and Barnard, 1984; Mooney, 1988). Supernatants were saved. For the second extraction of the serial extraction, pellets were carefully re-suspended in urea lysis buffer, incubated on ice for 15 minutes, and centrifuged as above. The resulting supernatants were collected and saved. Urea lysis buffer was modified based on the 4X LOX buffer previously described (Bertram and Hass, 2009), which contains 4.8 M urea and 200 mM sodium phosphate buffer [pH 7.4]. Western blots were performed as described previously (Chen et al., 2015). Densitometry of bands was analyzed with ImageJ (Schneider et al., 2012a).

Hydroxyproline Assay

The hydroxyproline contents in pellets obtained after the serial extraction described above were determined based on a modification of previously described protocols (Wells et al., 2009; Sousse et al., 2011; Cissell et al., 2017). Briefly, each pellet from the cells in a well of 6-well plate was resuspended in 100 μl 12 N HCl and vortexed. After hydrolysis, the samples were incubated at room temperature with 625 μl chloramine-T solution for 20 minutes, combined with 625 μl Ehrlich's solution at 65°C for 20 min, and cooled to room temperature. 200 μl from each tube was transferred to a 96-well plate in triplicate and optical density was measured at 550 nm, and the concentration of hydroxyproline was calculated against a standard curve (Wells et al., 2009; Sousse et al., 2011; Cissell et al., 2017).

Results

AEEA at micro molar concentration lacks in vitro cytotoxicity

MTT assays were performed in HTS fibroblasts as well as primary dermal fibroblasts isolated from non-burned skin of the same burn patient (NBS fibroblasts) and commercially available primary dermal fibroblasts from neonatal foreskin (PCS fibroblasts). The viability of the cells was calculated based on the optical density values that were normalized to that of the control (untreated) cells and expressed as a percentage of the control (Fig. 1), and the LC_{50} was determined using adjusted optical absorbance values (Table 1). These results are similar to those previously obtained in primary cultured rat aortic smooth muscle cells (Chen et al., 2015). Thus, AEEA concentrations used in subsequent experiments were far below the LC_{50}.

AEEA disrupted ECM structure in vitro

The effects of AEEA on ECM morphology were investigated in cultures of primary dermal fibroblasts (HTS fibroblasts) isolated from HS tissue from a burn patient. HTS fibroblasts were treated with AEEA (0.0, 25.0, 50.0, or 100.0 μM) for 14 days, and decellularized matrix scaffolds were prepared and analyzed via SEM. Cells treated with varying concentrations of AEEA appeared viable when observed under an optical microscope. Only rarely were dead cells seen (Fig. 2, top panel). Low-magnification (× 6000) SEM showed that the decellularized matrix scaffolds prepared from control (untreated) cells were integrated and relatively solid and compact, with a thin layer of discontinuous cell membrane being present at the surface of the ECM. At high magnification (× 60,000), the scaffolds appeared relatively flat, and some fibers could be clearly seen. In contrast, low magnification views of decellularized matrix scaffolds from AEEA-exposed cells revealed irregularities, the size and occurrence of which appeared to increase with increasing AEEA concentration (Fig. 2, middle panel, pointed out by arrowheads). The thin membrane present at the surface of ECM prepared from control cells was absent in ECM from AEEA-treated cells. High magnification views showed ECM fibers were considerably less abundant in cells exposed to 25.0 μM AEEA than in control cells, and fibers were not observed in ECM prepared from cells exposed to 50.0 to 100.0 μM AEEA (Fig. 2, lower panel). At high magnification, these increases in irregularities of ECM in a concentration dependent manner were also confirmed (Fig. 2, lower panel, pointed out by arrowheads). These results indicate

that AEEA alters the microstructure of ECM formed by HTS cells *in vitro* in a concentration-dependent manner.

AEEA increased the contact stiffness of ECM in vitro

To further quantify and better understand the effects of AEEA on ECM structure, we performed compression AFM (Fig. 3A) as described previously (Chen et al., 2015) to analyze the mechanical properties of ECM. Elastic deformation of ECM samples was determined using force-displacement curves for 2.5% agarose and glass as references (Fig. 3B). Glass is non-deformable, while 2.5% agarose has tissue-like elasticity, with a reported elastic (Young's) modulus of ~25 kPa as determined by AFM (Stolz et al., 2004; Loparic et al., 2010) and as confirmed here by fitting the contact region of the force-displacement curves using the Hertz model (25 ± 8 kPa). Fig. 3C shows force-displacement curves of ECM from HTS cells exposed to increasing concentrations of AEEA (0.0, 50.0, and 100.0 μM). We found that AEEA remarkably affected the nano-mechanics of the ECM. In untreated cells, ECM had a contact stiffness of 0.7 pN/nm, whereas a contact stiffness of 0.9 and 3.1 pN/nm in cells treated with 50.0 or 100.0 μM AEEA, respectively. These results suggest that AEEA causes a stiffening of the 3D nano-structure of the ECM.

AEEA increased the extractability of type I collagen protein

Type I collagen is a major component of skin and scar tissue, particularly HS tissue (Prockop and Kivirikko, 1995; Shoulders and Raines, 2009). To better understand the biochemical mechanisms underlying biophysical and micro-morphological aberrations in HTS fibroblast ECM, we performed Western blots to analyze the expression and extractability of type I collagen in HTS fibroblasts. This analysis was repeated in NBS and PCS fibroblasts to determine if AEEA causes similar alterations in human primary dermal fibroblasts from non-scar tissue. Fibroblasts were treated with varying concentrations of AEEA (0.0, 12.5, 25.0, 50.0, 100.0, or 250.0 μM) for 10 days and subjected to serial extractions. Proteins were then detected with antibody against type I collagen. Up to three bands were routinely detected. The intensities of the type I collagen bands increased in a dose-dependent manner in all three human primary dermal fibroblasts cell lines treated with AEEA (Fig. 4A). Next, we investigated time-dependent effects of AEEA on type I collagen extractability up to 14 days after 50.0 μM AEEA exposure. The intensities of the type I collagen bands increased in a time-dependent manner in the three cell lines treated with AEEA (Fig. 4B). These findings indicate that AEEA profoundly affects collagen extractability.

Effects of AEEA and TGF-β1 on the extractability and 3D structure of type I collagen

To investigate the effects of TGF-β1 and TGF-β1-AEEA interplay on collagen type I extractability, we performed Western blot analysis of serially extracted proteins from HTS fibroblasts treated with AEEA and/or TGF-β1. HTS fibroblasts were treated with AEEA (0.0 or 50.0 μM) and 4 days later, retreated with AEEA (0.0 or 50.0 μM) and/or TGF-β1 (0.0 or 2.5 ng/ml). At 7 days after AEEA treatment, native samples were prepared in digitonin lysis buffer, separated in denaturing gels, and probed with type I collagen antibody. In TGF-β1–treated cells, the extractability of type I collagen decreased slightly. In AEEA-treated cells, the intensity of the upper band increased slightly, that of the middle band was similar

to intensity of the control, and the intensity of the lower band decreased. In cells treated with both AEEA and TGF-β1, the intensities of the three bands were slightly greater than seen with TGF-β1 alone but slightly weaker than seen with AEEA alone, suggesting that AEEA countered the effects of TGF-β1 in the formation of ECM (Fig. 5 A, top panel).

Specific post-translational modifications to type I collagen are essential for the formation of functional fibrils (Kaku et al., 2007). TGF-β may induce expression of prolyl hydroxylase (Tsuji-Naito et al., 2010) and lysyl oxidase (Feres-Filho et al., 1995; Voloshenyuk et al., 2011), consequently alters the collagen post-translational modification and accelerates procollagen processing in cultured cells (Varga and Jimenez, 1986). These may result in changes in 3D structure, which may be identified by comparing the electrophoretic behavior of the protein (*i. e*, type I collagen) in denaturing gels and native gels. To this end, the native samples examined above were electrophoresed in native gels. When the native samples were separated in NuPAGE 7% Tris-Acetate native gel with the electrophoresis buffer in control sample, the upper band was more intense than the middle band, whereas the lower band was very faint. The two uppermost bands appeared as doublets or triplets (Fig. 5, middle panel, upper row). TGF-β1 exposure increased the intensity of the upper and lower band but decreased that of the middle band. An additional band was observed between the top and middle band that was not detected in the control, AEEA (50 μM), or AEEA (50 μM) + TGF-β1 (2.5 ng/ml) samples. In AEEA-treated cells, the intensity of the upper bands was lower than that of controls, but the middle and lower bands became slightly more intense. In cells co-treated with AEEA and TGF-β1, the intensities of the three bands were slightly lower than those seen with TGF-β1 alone but slightly greater than those seen with AEEA alone. When the native samples were separated in Native PAGE™ Novex™ 3-12% Bis-Tris protein gels with the electrophoresis buffer in the cathode tank contained 1.0% DOC, only one major band was detected with the type I collagen antibody and the GAPDH band was not detected. The overall changes of the intensity of the bands for type I collagen were similar to those seen with 0.2% DOC (Fig. 5 A, middle panel, lower row).

In summary, band intensities in samples extracted with digitonin were not consistent between the denaturing gel and native gel analyses. In TGF-β1–treated cells, the intensities of the three major bands decreased in the denaturing gels, but those of the upper and lower bands increased in the native gels. Whereas in AEEA–treated cells, the intensities of the upper band increased in the denaturing gels, but the band decreased in the native gels. This suggests that TGF-β1 and AEEA treatment affects the 3D structure of type I collagen protein molecules, possibly by altering post-translational modifications.

In urea buffer fraction, the extractability of the two lower type I collagen bands was decreased by TGF-β1 but increased by AEEA (Fig. 5A), indicating that both treatments altered the extractability of type I collagen. The antagonization effect of AEEA to TGF-β1 on ECM formation was also observed in this fraction, when compared the band intensities in the samples of cells treated with both AEEA and TGF-β1 to that of TGF-β1 or AEEA alone, which were consistent with that of the digitonin fraction described above.

Effects of AEEA and TGF-β1 on the collagen deposition in vitro

To test the effects of AEEA and TGF-β1 on the collagen deposition (Wells et al., 2009) in the *in vitro* formed ECM, the hydroxyproline in the pellets obtained after the serial extraction was quantified. Treatment with AEEA slightly increased the content of hydroxyproline, from 0.173 ± 0.006 mg/ml to 0.187 ± 0.015 mg/ml, which was approximately 7% increase when compared with that of the control samples. Treatment of TGF-β1 or the combination of TGF-β1 and AEEA did not change the content of hydroxyproline in the pellets (Fig. 5C).

Analysis of chemical structure–activity relationship

To search for agents chemically related to AEEA with more robust anti-fibrotic and anti-scarring properties, as well as to further investigate the molecular mechanisms underlying the effects of AEEA on ECM formation, we conducted studies of analogs of AEEA regarding a possible chemical structure–activity relationship (SAR). Such analyses enable identification of the chemical group, or key pharmacophore, responsible for eliciting any given biological effect (Perkins et al., 2003; Taylor et al., 2003; Carotenuto et al., 2006; Nantasenamat et al., 2010). We tested 12 commercially available chemical analogs of AEEA; all were modified at the hydroxyl or two amino functional groups. Extractability of type I collagen was analyzed in HTS fibroblasts exposed to 50 μM of analog for 10 days. Western blot data are shown for six analogs in Fig. 6A: diethylenetriamine (A1), diethanolamine (A2), 2-(2-(methylamino)-ethylamino)-ethanol (A3), triethanolamine (A4), 2-(2-aminoethoxy) ethanol (A5), and 2-(2-aminoethoxy) ethylamine (A6). Analysis of the native lysis buffer-extracted samples revealed that A1, A2, A4, and A5 slightly increased the intensity of the bands, particularly the lower bands, relative to the control. In samples re-extracted with urea lysis buffer, the intensities of the lower bands increased substantially in the samples from AEEA-, A1- and A6-treated cells (approximately 2.9-, 3.1- and 3.2- fold of that on the control, respectively) and drastically increased in samples from the cells treated with A5 (approximately 5.3-fold of that on the control). These data clearly show that altering the hydroxyl or amino pharmacophores affects activity and thus may guide rational drug design using such chemotypes as lead molecules.

The hydroxyproline contents in the pellets obtained after the serial extraction were quantified to test the effects of AEEA and its analogues on collagen deposition in the ECM formed *in vitro.* A4 and A6 slightly increased the contents of hydroxyproline 10 days post treatment, from 0.163 ± 0.008 mg/ml (Control) to 0.195 ± 0.034 mg/ml (A4) and 0.172 ± 0.008 mg/ml (A6), respectively (Fig. 6 C). Treatment of AEEA, A1, A2, A3 and A5 did not change the contents of hydroxyproline.

Discussion

Developing innovative effective pharmacologic therapies for the prevention and treatment of HS in burn rehabilitation is essential, since none is currently available other than surgical resection. The cutaneous ECM not only serves as a structural scaffold, but also has multiple physiological roles, including storage and delivery of growth factors and cytokines and tissue repair. Wound healing and the progression of fibrosis are tightly controlled by the

assembly, composition, and hierarchical architecture of the ECM. Abnormal reconstruction of the ECM and increased deposition of ECM proteins, particularly collagen (Midwood et al., 2004; Myllyharju and Kivirikko, 2004; van der Veer et al., 2009; Reinke and Sorg, 2012; Carver and Goldsmith, 2013; Mouw et al., 2014; Zgheib et al., 2014; Xue and Jackson, 2015), and increase of the cross-linking of collagen (Moriguchi and Fujimoto, 1979; Cohen, 1985; Uzawa et al., 1998; van den Bogaerdt et al., 2009) contribute to HS formation. Thus, blocking excessive formation of ECM and the cross-linking of collagen during the remodeling phase of wound healing may reduce the abnormal scarring that results in HS.

To determine whether AEEA possesses potential anti-scar properties, we first investigated the effects of AEEA on the morphology of the ECM formed by human HTS fibroblasts *in vitro.* Cultured dermal fibroblasts can produce ECM, and an ECM sheet can be observed when cells are scraped with a cell lifter or scraper. In our studies, cultured human dermal fibroblasts usually produced a thin ECM sheet approximately 7 days after cell seeding. The ECM sheet then became thicker gradually by up to approximately 2 weeks (the longest time examined in this study) and could be examined via scanning electron microscopy and atomic force microscopy. Therefore, cultured dermal fibroblasts provide a convenient system for studying aberrations in collagen metabolism (Booth et al., 1980; Uitto et al., 1980; Booth and Uitto, 1981) and ECM formation under a variety of conditions *in vitro,* as illustrated by our previous study of *in vivo* and *in vitro* vascular ECM formation (Chen et al., 2015). While animal models provide a useful approach for studying the mechanisms underlying HS formation, *in vitro* models offer many advantages, such as providing a simpler system for investigation of a small number of issues. Studying human cell lines also eliminates species bias. Furthermore, cell models can be adapted for high-throughput screening of molecules with pharmacological or toxicological activity.

Similar to our previous studies on rat aorta smooth muscle cells (Chen et al., 2015), this study relied on micromolar concentrations of AEEA which were far below the LC_{50} determined by MTT assay (e.g., in the range of 18.26 to 25.25 mM). Visual inspection under an optical microscope showed that, for all three human dermal fibroblast types, most cells treated with micromolar AEEA concentrations appeared unchanged in morphology or growth for up to 2 weeks.

SEM revealed that treatment with AEEA markedly altered the structure of the ECM produced *in vitro.* More irregularities were present, and AEEA decreased the number of fibers in a dose-dependent manner, suggesting that AEEA hinders ECM formation. In addition, a thin layer of what appeared to be a possible cell membrane was observed at the surface of the ECM prepared from control cells but not AEEA-treated cells, suggesting that AEEA decreases the binding of cell membrane to the ECM, which remains to be further determined.

Next, AFM indentation studies were performed to determine the effect of AEEA on the biophysical properties of ECM formed by HTS fibroblasts *in vitro.* These studies revealed that AEEA had a considerable effect on the mechanical properties of ECM produced by cultured HTS fibroblasts. Specifically, they suggested that AEEA induces marked stiffening of the ECM. Since the AFM tip is smaller than the diameter of a collagen fiber, the reduction

in the deformability suggests that the ECM nano-structure was altered, perhaps as a result of a change in the 3D organization of collagen-elastin network. Understanding how such a decrease in deformability is associated with changes in the interstitial matrix of the ECM in HS should be a goal of future studies.

Collagens are the most abundant macromolecules in the ECM and have versatile physiologic roles ranging from providing structural support to mediating cell signaling. Collagen is involved in all 3 phases of the wound-healing cascade (Fleck and Simman, 2010). Type I collagen is the major component of skin and scar tissue, including HS (Prockop and Kivirikko, 1984; Prockop and Kivirikko, 1995; Shoulders and Raines, 2009). Deposition of excess collagen results in a pathological scar (Tredget et al., 2014; Zgheib et al., 2014). Western blot analysis of type I collagen was performed in HTS fibroblasts and two other human primary dermal fibroblasts cell lines (NBS and PCS fibroblasts) to investigate the biochemical mechanisms underlying biophysical and micro-morphological aberrations in HS ECM. Type I collagen extractability may depend on the strength of detergents in the lysis buffers and intermolecular protein interactions, which are associated with post-translational modification (Kivirikko and Myllyla, 1982; Kivirikko and Myllyla, 1987; Koivu, 1987; Prockop and Kivirikko, 1995; Kivirikko and Pihlajaniemi, 1998; Jurgensen et al., 2011; Yamauchi and Sricholpech, 2012; Perdivara et al., 2013; Terajima et al., 2014; Gjaltema and Bank, 2017). The results showed that AEEA increased the extractability of type I collagen in a dose- and time-dependent fashion, particularly in urea (Pace, 1986; Bennion and Daggett, 2003; Hua et al., 2008; Li et al., 2012) fractions, perhaps by interfering with intermolecular interactions and/or crosslinking within the collagen molecule.

Collagen is post-translationally modified in several ways (Prockop and Kivirikko, 1995; Myllyharju and Kivirikko, 2004; Gjaltema and Bank, 2017): 1) Signal peptides that direct the pre-pro-peptide into the endoplasmic reticulum are cleaved. 2) Lysyl hydroxylase hydroxylates lysine residues (Kivirikko and Pihlajaniemi, 1998); and 3) prolyl hydroxylase hydroxylates proline residues (Smith and Talbot, 2010). 4) Some hydroxylysine residues undergo glycosylation to form galactosylhydroxylysine and glucosylgalactosylhydroxylysine, and certain asparagine residues in the C propeptides or some in both the N and C propeptides undergo glycosylation (Butler and Cunningham, 1966; Kivirikko and Myllyla, 1982; Kivirikko and Myllyla, 1987; Myllyharju and Kivirikko, 2001; Yamauchi and Sricholpech, 2012; Perdivara et al., 2013; Terajima et al., 2014). 5) Intermolecular disulphide bonds also form (Bernard et al., 1983; Koivu, 1987; Pace et al., 2001; Pawelec et al., 2016). Glycosylation is a very important post-translational modification of collagen (Perdivara et al., 2013). Collagen glycosylation is thought to play a key role in regulating its crosslinking. Glycosylation may facilitate interactions between collagen and other molecules, increase collagen resistance to proteolytic degradation, and regulate lateral growth of collagen fibrils (Vogel et al., 1997; Bhadriraju et al., 2009; Jurgensen et al., 2011; Xu et al., 2011; Yamauchi and Sricholpech, 2012). Glycan in fibrillar collagen also serves as a ligand for collagen-specific cell-surface receptors, such as discoidin domain receptors 1 and 2 (Vogel et al., 1997; Bhadriraju et al., 2009; Jurgensen et al., 2011; Xu et al., 2011; Que et al., 2015); in this way, glycan regulates certain signaling pathways. In denaturing gels, the presence of anionic detergents such as SDS may linearize proteins

and impart a negative charge (Shapiro et al., 1967; Reynolds and Tanford, 1970). In addition, reducing agents may disrupt the disulfide bonds of protein and then further linearize the proteins. On the other hand, in clear-native PAGE, proteins are folded or assembled so that the physical size of the 3D protein, individual molecule, or protein complex as well as the electric charge at the surface of protein affects its mobility (Wittig and Schagger, 2005; Wittig and Schagger, 2008). Therefore, the electrophoretic behavior of a native protein may differ from that of a denatured protein. The presence of DOC in the cathode buffer may be advantageous for detecting proteins in clear-native PAGE (Ladig et al., 2011). In our experience, the concentration of DOC in the electrophoresis buffer markedly affects the electrophoretic behavior of native collagen. In the absence of DOC, no type I collagen bands were detected, but only smears. At 0.2% DOC, three major bands of type I collagen were easily detected, and a GAPDH band was evident, whereas at a higher DOC concentration (1%), only one major band of collagen type I was detected, and the GAPDH band became undetectable. Different DOC concentrations, particularly those below the critical micelle concentration, *e.g.,* less than 5 mM (Matsuoka et al., 2013), may affect the intramolecular and intermolecular interactions of the collagen protein to a different extent, resulting in differing 3D structures and electrophoretic behaviors of native collagen protein.

In our experiments, cells were seed at higher densities, i.e., were confluent on the next day. After extractions, wet weight of each pellet obtained when cells were harvested 10 to 14 days post treatment was approximately 12~16 mg/well, and the size of pellets among the different treated cells in the same batch of experiments looked quite similar. The digitonin and urea fraction usually contain approximately 400~600 μg and 80~100 μg total protein/well, respectively. In the denaturing gels, treatment with TGFβ1 caused a decrease of intensity of collagen type I bands. This decrease could be due to less extractability of collagen type I. Treatment with TGFβ1 did not increase the collagen deposition, which suggests that the extractable collagen in the two fractions (digitonin and urea) could be only a small portion of the total collagen. Also, most of the collagen could be in the cross-linked form, and thus would remain in the pellets after extraction.

SAR analysis enables identification of the chemical group underlying any given biological effect in an organism or cells. This allows one to optimize the biological effect by changing the chemical structure. For example, one can increase the potency and reduce the toxicity and/or side-effects of a bioactive compound by replacing the chemical groups or inserting new ones (Taylor et al., 2003; Carotenuto et al., 2006; Nantasenamat et al., 2010). AEEA was not found to be genotoxic in tests for gene mutation, chromosomal aberrations, sister chromatid exchange, or unscheduled DNA synthesis in bacteria and mammalian cells *in vitro* (Leung, 1994). Although it is extensively used in industry as a chemical intermediate (Moore et al., 2012; Schneider et al., 2012b), the potential toxicity of AEEA to human remains to be investigated. However, AEEA induced dissecting aortic aneurysm in the offspring of rats during gestation and early lactation (Moore et al., 2012; Schneider et al., 2012b; Xu et al., 2014; Chen et al., 2015). In addition, at higher concentration, *i.e.,* 1% (approximately 96 mM, which is much higher than the μM concentration used in this study), AEEA may be a skin sensitizer (Foti et al., 2001). This study shows that altering the hydroxyl or amino pharmacophores affects activity and thus, that a SAR exists. Future

investigation of specifically designed analogs may guide rational chemical design and lead to the discovery of drugs that effectively reduce hypertrophic scarring.

AEEA did not increase collagen deposition when cells were treated for 10 days, although it slightly increased the hydroxyproline content when cells were treated for 7 days. The mechanisms of these paradoxical phenomena remains to be further studied. Among the 6 AEEA analogues, 4 did not change collagen deposition, whereas 2 of them (A4 and A6) slightly increased the collagen deposition. These data suggest that these chemicals may cause changes of post-translational modifications of collagen, but not collagen synthesis *in vitro.* The detail changes of post-translational modifications of collagen and how they would affect HTS formation remain to be further investigated.

To conclude, these *in vitro* studies showed that non-toxic micromolar concentrations of AEEA may alter the micro-3D structure of the ECM produced by cultured HTS fibroblasts as observed by SEM. AEEA also made the ECM stiffer, and less deformable, as seen by AFM. Western blot analyses showed that AEEA increased the extractability of type I collagen in a dose- and time-dependent fashion. The difference of the electrophoretic behavior of the same set of samples under native and denaturing conditions suggested that AEEA alters the 3D structure of type I collagen. These findings indicate that AEEA has a profound effect on collagen metabolism, perhaps owing to its ability to alter the intramolecular and intermolecular interactions of the collagen molecule. Data obtained here from SAR analyses suggest that further search and design of AEEA analogs are promising strategies for developing new therapies for hypertrophic scarring. Future studies of AEEA will focus on potential therapeutic effects of this or similar agents.

Acknowledgments

This project was supported by grants from the National Institutes of Health (R21-ES-013038 and R21-ES-022821 to PJB, R01-GM-056687 and P50-GM-060338 to DNH, and R01-GM-112936 to CCF) and grants from Shriners Hospitals for Children (71000 and 84080 to DNH, and 71001 to CCF). We thank BASF SE (Ludwigshafen, Germany) for the kind donation of AEEA, and Dr. Kasie Cole for editing and proofreading this manuscript.

Abbreviations:

AEEA	N-(2-Aminoethyl) Ethanolamine
AFM	atomic force microscopy
ECM	extracellular matrix
HS	hypertrophic scar
HTS fibroblast	hypertrophic scar fibroblast
NBS fibroblast	non-burned skin fibroblast
PCS	commercially available human primary dermal fibroblasts obtained from normal neonatal foreskin
SAR	chemical structure–activity relationship

SEM	scanning electron microscopy

References

Annes JP, Munger JS, Rifkin DB, 2003 Making sense of latent TGFbeta activation. J Cell Sci 116, 217–224. [PubMed: 12482908]

Armour A, Scott PG, Tredget EE, 2007 Cellular and molecular pathology of HTS: basis for treatment. Wound Repair Regen 15 Suppl 1, S6–17. [PubMed: 17727469]

Bennion BJ, Daggett V, 2003 The molecular basis for the chemical denaturation of proteins by urea. Proc Natl Acad Sci U S A 100, 5142–5147. [PubMed: 12702764]

Bernard MP, Myers JC, Chu ML, Ramirez F, Eikenberry EF, Prockop DJ, 1983 Structure of a cDNA for the pro alpha 2 chain of human type I procollagen. Comparison with chick cDNA for pro alpha 2(I) identifies structurally conserved features of the protein and the gene. Biochemistry 22, 1139–1145. [PubMed: 6687691]

Bertram C, Hass R, 2009 Cellular senescence of human mammary epithelial cells (HMEC) is associated with an altered MMP-7/HB-EGF signaling and increased formation of elastin-like structures. Mech Ageing Dev 130, 657–669. [PubMed: 19682489]

Bhadriraju K, Chung KH, Spurlin TA, Haynes RJ, Elliott JT, Plant AL, 2009 The relative roles of collagen adhesive receptor DDR2 activation and matrix stiffness on the downregulation of focal adhesion kinase in vascular smooth muscle cells. Biomaterials 30, 6687–6694. [PubMed: 19762078]

Blobe GC, Schiemann WP, Lodish HF, 2000 Role of transforming growth factor beta in human disease. N Engl J Med 342, 1350–1358. [PubMed: 10793168]

Bombaro KM, Engrav LH, Carrougher GJ, Wiechman SA, Faucher L, Costa BA, Heimbach DM, Rivara FP, Honari S, 2003 What is the prevalence of hypertrophic scarring following burns? Burns 29, 299–302. [PubMed: 12781605]

Boo S, Dagnino L, 2013 Integrins as Modulators of Transforming Growth Factor Beta Signaling in Dermal Fibroblasts During Skin Regeneration After Injury. Adv Wound Care (New Rochelle) 2, 238–246. [PubMed: 24527345]

Booth BA, Polak KL, Uitto J, 1980 Collagen biosynthesis by human skin fibroblasts. I. Optimization of the culture conditions for synthesis of type I and type III procollagens. Biochim Biophys Acta 607, 145–160. [PubMed: 7370260]

Booth BA, Uitto J, 1981 Collagen biosynthesis by human skin fibroblasts. III. The effects of ascorbic acid on procollagen production and prolyl hydroxylase activity. Biochim Biophys Acta 675, 117–122. [PubMed: 6266492]

Butler WT, Cunningham LW, 1966 Evidence for the linkage of a disaccharide to hydroxylysine in tropocollagen. J Biol Chem 241, 3882–3888. [PubMed: 4288358]

Butzelaar L, Ulrich MM, Mink van der Molen AB, Niessen FB, Beelen RH, 2016 Currently known risk factors for hypertrophic skin scarring: A review. J Plast Reconstr Aesthet Surg 69, 163–169. [PubMed: 26776348]

Carotenuto A, D'Ursi AM, Mulinacci B, Paolini I, Lolli F, Papini AM, Novellino E, Rovero P, 2006 Conformation-activity relationship of designed glycopeptides as synthetic probes for the detection of autoantibodies, biomarkers of multiple sclerosis. J Med Chem 49, 5072–5079. [PubMed: 16913697]

Carver W, Goldsmith EC, 2013 Regulation of tissue fibrosis by the biomechanical environment. Biomed Res Int 2013, 101979. [PubMed: 23781495]

Chen Z, Xu Y, Bujalowski P, Oberhauser AF, Boor PJ, 2015 N-(2-Aminoethyl) Ethanolamine-Induced Morphological, Biochemical, and Biophysical Alterations in Vascular Matrix Associated With Dissecting Aortic Aneurysm. Toxicol Sci 148, 421–432. [PubMed: 26443843]

Cissell DD, Link JM, Hu JC, Athanasiou KA, 2017 A Modified Hydroxyproline Assay Based on Hydrochloric Acid in Ehrlich's Solution Accurately Measures Tissue Collagen Content. Tissue Eng Part C Methods 23, 243–250. [PubMed: 28406755]

Cohen IK, 1985 Can collagen metabolism be controlled: theoretical considerations. J Trauma 25, 410–412. [PubMed: 3923206]

Dallas SL, Sivakumar P, Jones CJ, Chen Q, Peters DM, Mosher DF, Humphries MJ, Kielty CM, 2005 Fibronectin regulates latent transforming growth factor-beta (TGF beta) by controlling matrix assembly of latent TGF beta-binding protein-1. J Biol Chem 280, 18871–18880. [PubMed: 15677465]

Davidson JM, LuValle PA, Zoia O, Quaglino D Jr., Giro M, 1997 Ascorbate differentially regulates elastin and collagen biosynthesis in vascular smooth muscle cells and skin fibroblasts by pretranslational mechanisms. J Biol Chem 272, 345–352. [PubMed: 8995268]

Deitch EA, Wheelahan TM, Rose MP, Clothier J, Cotter J, 1983 Hypertrophic burn scars: analysis of variables. J Trauma 23, 895–898. [PubMed: 6632013]

Demoliou-Mason CD, Barnard EA, 1984 Solubilization in high yield of opioid receptors retaining high-affinity delta, mu and kappa binding sites. FEBS Lett 170, 378–382. [PubMed: 6144572]

Feres-Filho EJ, Choi YJ, Han X, Takala TE, Trackman PC, 1995 Pre- and post-translational regulation of lysyl oxidase by transforming growth factor-beta 1 in osteoblastic MC3T3-E1 cells. J Biol Chem 270, 30797–30803. [PubMed: 8530522]

Finnerty CC, Jeschke MG, Branski LK, Barret JP, Dziewulski P, Herndon DN, 2016 Hypertrophic scarring: the greatest unmet challenge after burn injury. Lancet 388, 1427–1436. [PubMed: 27707499]

Finnson KW, Arany PR, Philip A, 2013 Transforming Growth Factor Beta Signaling in Cutaneous Wound Healing: Lessons Learned from Animal Studies. Adv Wound Care (New Rochelle) 2, 225–237. [PubMed: 24761336]

Fleck CA, Simman R, 2010 Modern collagen wound dressings: function and purpose. J Am Col Certif Wound Spec 2, 50–54. [PubMed: 24527149]

Foti C, Bonamonte D, Mascolo G, Tiravanti G, Rigano L, Angelini G, 2001 Aminoethylethanolamine: a new allergen in cosmetics? Contact Dermatitis 45, 129–133. [PubMed: 11553136]

Gabriel V, 2011 Hypertrophic scar. Phys Med Rehabil Clin N Am 22, 301–310, vi. [PubMed: 21624722]

Gauglitz GG, Korting HC, Pavicic T, Ruzicka T, Jeschke MG, 2011 Hypertrophic scarring and keloids: pathomechanisms and current and emerging treatment strategies. Mol Med 17, 113–125. [PubMed: 20927486]

Gjaltema RA, Bank RA, 2017 Molecular insights into prolyl and lysyl hydroxylation of fibrillar collagens in health and disease. Crit Rev Biochem Mol Biol 52, 74–95. [PubMed: 28006962]

He NG, Awasthi S, Singhal SS, Trent MB, Boor PJ, 1998 The role of glutathione S-transferases as a defense against reactive electrophiles in the blood vessel wall. Toxicol Appl Pharmacol 152, 83–89. [PubMed: 9772203]

Hinz B, 2015 The extracellular matrix and transforming growth factor-beta1: Tale of a strained relationship. Matrix Biol 47, 54–65. [PubMed: 25960420]

Hinz B, 2016 Myofibroblasts. Exp Eye Res 142, 56–70. [PubMed: 26192991]

Hua L, Zhou R, Thirumalai D, Berne BJ, 2008 Urea denaturation by stronger dispersion interactions with proteins than water implies a 2-stage unfolding. Proc Natl Acad Sci U S A 105, 16928–16933. [PubMed: 18957546]

Jurgensen HJ, Madsen DH, Ingvarsen S, Melander MC, Gardsvoll H, Patthy L, Engelholm LH, Behrendt N, 2011 A novel functional role of collagen glycosylation: interaction with the endocytic collagen receptor uparap/ENDO180. J Biol Chem 286, 32736–32748. [PubMed: 21768090]

Kaku M, Mochida Y, Atsawasuwan P, Parisuthiman D, Yamauchi M, 2007 Post-translational modifications of collagen upon BMP-induced osteoblast differentiation. Biochem Biophys Res Commun 359, 463–468. [PubMed: 17553463]

Kivirikko KI, Myllyla R, 1982 Posttranslational enzymes in the biosynthesis of collagen: intracellular enzymes. Methods Enzymol 82 Pt A, 245–304. [PubMed: 6210830]

Kivirikko KI, Myllyla R, 1987 Recent developments in posttranslational modification: intracellular processing. Methods Enzymol 144, 96–114. [PubMed: 3041180]

Kivirikko KI, Pihlajaniemi T, 1998 Collagen hydroxylases and the protein disulfide isomerase subunit of prolyl 4-hydroxylases. Adv Enzymol Relat Areas Mol Biol 72, 325–398. [PubMed: 9559057]

Koivu J, 1987 Identification of disulfide bonds in carboxy-terminal propeptides of human type I procollagen. FEBS Lett 212, 229–232. [PubMed: 3817157]

Ladig R, Sommer MS, Hahn A, Leisegang MS, Papasotiriou DG, Ibrahim M, Elkehal R, Karas M, Zickermann V, Gutensohn M, Brandt U, Klosgen RB, Schleiff E, 2011 A high-definition native polyacrylamide gel electrophoresis system for the analysis of membrane complexes. Plant J 67, 181–194. [PubMed: 21418111]

Leask A, Abraham DJ, 2004 TGF-beta signaling and the fibrotic response. FASEB J 18, 816–827. [PubMed: 15117886]

Leung HW, 1994 Evaluation of the genotoxic potential of alkyleneamines. Mutat Res 320, 31–43. [PubMed: 7506385]

Li W, Zhou R, Mu Y, 2012 Salting effects on protein components in aqueous NaCl and urea solutions: toward understanding of urea-induced protein denaturation. J Phys Chem B 116, 1446–1451. [PubMed: 22216970]

Loparic M, Wirz D, Daniels AU, Raiteri R, Vanlandingham MR, Guex G, Martin I, Aebi U, Stolz M, 2010 Micro- and nanomechanical analysis of articular cartilage by indentation-type atomic force microscopy: validation with a gel-microfiber composite. Biophys J 98, 2731–2740. [PubMed: 20513418]

Matsuoka K, Takagi K, Honda C, 2013 Micelle formation of sodium hyodeoxycholate. Chem Phys Lipids 172–173, 6–13.

Midwood KS, Williams LV, Schwarzbauer JE, 2004 Tissue repair and the dynamics of the extracellular matrix. Int J Biochem Cell Biol 36, 1031–1037. [PubMed: 15094118]

Mooney RA, 1988 Use of digitonin-permeabilized adipocytes for cAMP studies. Methods Enzymol 159, 193–202. [PubMed: 2842586]

Moore NP, Tornesi B, Yano BL, Nitschke KD, Carney EW, 2012 Developmental sensitivity to the induction of great vessel malformations by N-(2-aminoethyl)ethanolamine. Birth Defects Res B Dev Reprod Toxicol 95, 116–122. [PubMed: 22447736]

Moriguchi T, Fujimoto D, 1979 Crosslink of collagen in hypertrophic scar. J Invest Dermatol 72, 143–145. [PubMed: 422877]

Moustakas A, Pardali K, Gaal A, Heldin CH, 2002 Mechanisms of TGF-beta signaling in regulation of cell growth and differentiation. Immunol Lett 82, 85–91. [PubMed: 12008039]

Mouw JK, Ou G, Weaver VM, 2014 Extracellular matrix assembly: a multiscale deconstruction. Nat Rev Mol Cell Biol 15, 771–785. [PubMed: 25370693]

Myllyharju J, Kivirikko KI, 2001 Collagens and collagen-related diseases. Ann Med 33, 7–21. [PubMed: 11310942]

Myllyharju J, Kivirikko KI, 2004 Collagens, modifying enzymes and their mutations in humans, flies and worms. Trends Genet 20, 33–43. [PubMed: 14698617]

Nall AV, Brownlee RE, Colvin CP, Schultz G, Fein D, Cassisi NJ, Nguyen T, Kalra A, 1996 Transforming growth factor beta 1 improves wound healing and random flap survival in normal and irradiated rats. Arch Otolaryngol Head Neck Surg 122, 171–177. [PubMed: 8630211]

Nantasenamat C, Isarankura-Na-Ayudhya C, Prachayasittikul V, 2010 Advances in computational methods to predict the biological activity of compounds. Expert Opin Drug Discov 5, 633–654. [PubMed: 22823204]

Nunes I, Gleizes PE, Metz CN, Rifkin DB, 1997 Latent transforming growth factor-beta binding protein domains involved in activation and transglutaminase-dependent cross-linking of latent transforming growth factor-beta. J Cell Biol 136, 1151–1163. [PubMed: 9060478]

Oberhauser AF, Marszalek PE, Erickson HP, Fernandez JM, 1998 The molecular elasticity of the extracellular matrix protein tenascin. Nature 393, 181–185. [PubMed: 9603523]

Pace CN, 1986 Determination and analysis of urea and guanidine hydrochloride denaturation curves. Methods Enzymol 131, 266–280. [PubMed: 3773761]

Pace JM, Kuslich CD, Willing MC, Byers PH, 2001 Disruption of one intra-chain disulphide bond in the carboxyl-terminal propeptide of the proalpha1(I) chain of type I procollagen permits slow assembly and secretion of overmodified, but stable procollagen trimers and results in mild osteogenesis imperfecta. J Med Genet 38, 443–449. [PubMed: 11432962]

Pawelec KM, Best SM, Cameron RE, 2016 Collagen: a network for regenerative medicine. J Mater Chem B Mater Biol Med 4, 6484–6496. [PubMed: 27928505]

Penn JW, Grobbelaar AO, Rolfe KJ, 2012 The role of the TGF-beta family in wound healing, burns and scarring: a review. Int J Burns Trauma 2, 18–28. [PubMed: 22928164]

Perdivara I, Yamauchi M, Tomer KB, 2013 Molecular Characterization of Collagen Hydroxylysine O-Glycosylation by Mass Spectrometry: Current Status. Aust J Chem 66, 760–769. [PubMed: 25414518]

Perkins R, Fang H, Tong W, Welsh WJ, 2003 Quantitative structure-activity relationship methods: perspectives on drug discovery and toxicology. Environ Toxicol Chem 22, 1666–1679. [PubMed: 12924569]

Piek E, Ju WJ, Heyer J, Escalante-Alcalde D, Stewart CL, Weinstein M, Deng C, Kucherlapati R, Bottinger EP, Roberts AB, 2001 Functional characterization of transforming growth factor beta signaling in Smad2- and Smad3-deficient fibroblasts. J Biol Chem 276, 19945–19953. [PubMed: 11262418]

Pinnel SR, Murad S, Darr D, 1987 Induction of collagen synthesis by ascorbic acid. A possible mechanism. Arch Dermatol 123, 1684–1686. [PubMed: 2825607]

Pinnell SR, 1985 Regulation of collagen biosynthesis by ascorbic acid: a review. Yale J Biol Med 58, 553–559. [PubMed: 3008449]

Prockop DJ, Kivirikko KI, 1984 Heritable diseases of collagen. N Engl J Med 311, 376–386. [PubMed: 6146097]

Prockop DJ, Kivirikko KI, 1995 Collagens: molecular biology, diseases, and potentials for therapy. Annu Rev Biochem 64, 403–434. [PubMed: 7574488]

Que RA, Chan SW, Jabaiah AM, Lathrop RH, Da Silva NA, Wang SW, 2015 Tuning cellular response by modular design of bioactive domains in collagen. Biomaterials 53, 309–317. [PubMed: 25890729]

Rabello FB, Souza CD, Farina Junior JA, 2014 Update on hypertrophic scar treatment. Clinics (Sao Paulo) 69, 565–573. [PubMed: 25141117]

Reinke JM, Sorg H, 2012 Wound repair and regeneration. Eur Surg Res 49, 35–43. [PubMed: 22797712]

Reynolds JA, Tanford C, 1970 Binding of dodecyl sulfate to proteins at high binding ratios. Possible implications for the state of proteins in biological membranes. Proc Natl Acad Sci U S A 66, 1002–1007. [PubMed: 5269225]

Rhett JM, Ghatnekar GS, Palatinus JA, O'Quinn M, Yost MJ, Gourdie RG, 2008 Novel therapies for scar reduction and regenerative healing of skin wounds. Trends Biotechnol 26, 173–180. [PubMed: 18295916]

Roberts AB, Heine UI, Flanders KC, Sporn MB, 1990 Transforming growth factor-beta. Major role in regulation of extracellular matrix. Ann N Y Acad Sci 580, 225–232. [PubMed: 2186691]

Roberts AB, Sporn MB, Assoian RK, Smith JM, Roche NS, Wakefield LM, Heine UI, Liotta LA, Falanga V, Kehrl JH, et al., 1986 Transforming growth factor type beta: rapid induction of fibrosis and angiogenesis in vivo and stimulation of collagen formation in vitro. Proc Natl Acad Sci U S A 83, 4167–4171. [PubMed: 2424019]

Schneider CA, Rasband WS, Eliceiri KW, 2012a NIH Image to ImageJ: 25 years of image analysis. Nat Methods 9, 671–675. [PubMed: 22930834]

Schneider S, Treumann S, Moore NP, 2012b Malformations of the great vessels in the neonatal rat induced by N-(2-aminoethyl)ethanolamine. Birth Defects Res B Dev Reprod Toxicol 95, 95–106. [PubMed: 22461421]

Scott PG, Ghahary A, Tredget EE, 2000 Molecular and cellular aspects of fibrosis following thermal injury. Hand Clin 16, 271–287. [PubMed: 10791173]

Shapiro AL, Vinuela E, Maizel JV Jr., 1967 Molecular weight estimation of polypeptide chains by electrophoresis in SDS-polyacrylamide gels. Biochem Biophys Res Commun 28, 815–820. [PubMed: 4861258]

Sheridan RL, Tompkins RG, 2004 What's new in burns and metabolism. J Am Coll Surg 198, 243–263. [PubMed: 14759783]

Shoulders MD, Raines RT, 2009 Collagen structure and stability. Annu Rev Biochem 78, 929–958. [PubMed: 19344236]

Smith TG, Talbot NP, 2010 Prolyl hydroxylases and therapeutics. Antioxid Redox Signal 12, 431–433. [PubMed: 19761407]

Sousse LE, Yamamoto Y, Enkhbaatar P, Rehberg SW, Wells SM, Leonard S, Traber MG, Yu YM, Cox RA, Hawkins HK, Traber LD, Herndon DN, Traber DL, 2011 Acute lung injury-induced collagen deposition is associated with elevated asymmetric dimethylarginine and arginase activity. Shock 35, 282–288. [PubMed: 20938379]

Stolz M, Raiteri R, Daniels AU, VanLandingham MR, Baschong W, Aebi U, 2004 Dynamic elastic modulus of porcine articular cartilage determined at two different levels of tissue organization by indentation-type atomic force microscopy. Biophys J 86, 3269–3283. [PubMed: 15111440]

Taipale J, Saharinen J, Hedman K, Keski-Oja J, 1996 Latent transforming growth factor-beta 1 and its binding protein are components of extracellular matrix microfibrils. J Histochem Cytochem 44, 875–889. [PubMed: 8756760]

Taylor RE, Chen Y, Beatty A, Myles DC, Zhou Y, 2003 Conformation-activity relationships in polyketide natural products: a new perspective on the rational design of epothilone analogues. J Am Chem Soc 125, 26–27. [PubMed: 12515494]

Terajima M, Perdivara I, Sricholpech M, Deguchi Y, Pleshko N, Tomer KB, Yamauchi M, 2014 Glycosylation and cross-linking in bone type I collagen. J Biol Chem 289, 22636–22647. [PubMed: 24958722]

Tredget EE, Levi B, Donelan MB, 2014 Biology and principles of scar management and burn reconstruction. Surg Clin North Am 94, 793–815. [PubMed: 25085089]

Tsuji-Naito K, Ishikura S, Akagawa M, Saeki H, 2010 alpha-Lipoic acid induces collagen biosynthesis involving prolyl hydroxylase expression via activation of TGF-beta-Smad signaling in human dermal fibroblasts. Connect Tissue Res 51, 378–387. [PubMed: 20604712]

Uitto J, Booth BA, Polak KL, 1980 Collagen biosynthesis by human skin fibroblasts. II. Isolation and further characterization of type I and type III procollagens synthesized in culture. Biochim Biophys Acta 624, 545–561. [PubMed: 7417491]

Uzawa K, Marshall MK, Katz EP, Tanzawa H, Yeowell HN, Yamauchi M, 1998 Altered posttranslational modifications of collagen in keloid. Biochem Biophys Res Commun 249, 652–655. [PubMed: 9731191]

van den Bogaerdt AJ, van der Veen VC, van Zuijlen PP, Reijnen L, Verkerk M, Bank RA, Middelkoop E, Ulrich MM, 2009 Collagen cross-linking by adipose-derived mesenchymal stromal cells and scar-derived mesenchymal cells: Are mesenchymal stromal cells involved in scar formation? Wound Repair Regen 17, 548–558. [PubMed: 19614920]

van der Veer WM, Bloemen MC, Ulrich MM, Molema G, van Zuijlen PP, Middelkoop E, Niessen FB, 2009 Potential cellular and molecular causes of hypertrophic scar formation. Burns 35, 15–29. [PubMed: 18952381]

Varga J, Jimenez SA, 1986 Stimulation of normal human fibroblast collagen production and processing by transforming growth factor-beta. Biochem Biophys Res Commun 138, 974–980. [PubMed: 3461787]

Vogel W, Gish GD, Alves F, Pawson T, 1997 The discoidin domain receptor tyrosine kinases are activated by collagen. Mol Cell 1, 13–23. [PubMed: 9659899]

Voloshenyuk TG, Landesman ES, Khoutorova E, Hart AD, Gardner JD, 2011 Induction of cardiac fibroblast lysyl oxidase by TGF-beta1 requires PI3K/Akt, Smad3, and MAPK signaling. Cytokine 55, 90–97. [PubMed: 21498085]

Wells SM, Buford MC, Migliaccio CT, Holian A, 2009 Elevated asymmetric dimethylarginine alters lung function and induces collagen deposition in mice. Am J Respir Cell Mol Biol 40, 179–188. [PubMed: 18703795]

Wittig I, Schagger H, 2005 Advantages and limitations of clear-native PAGE. Proteomics 5, 4338–4346. [PubMed: 16220535]

Wittig I, Schagger H, 2008 Features and applications of blue-native and clear-native electrophoresis. Proteomics 8, 3974–3990. [PubMed: 18763698]

Wurzer P, Forbes AA, Hundeshagen G, Andersen CR, Epperson KM, Meyer WJ 3rd, Kamolz LP, Branski LK, Suman OE, Herndon DN, Finnerty CC, 2017 Two-year follow-up of outcomes

related to scarring and distress in children with severe burns. Disabil Rehabil 39, 1639–1643. [PubMed: 27685196]

Xie JL, Qi SH, Pan S, Xu YB, Li TZ, Liu XS, Liu P, 2008 Expression of Smad protein by normal skin fibroblasts and hypertrophic scar fibroblasts in response to transforming growth factor beta1. Dermatol Surg 34, 1216–1224; discussion 1224–1215. [PubMed: 18616749]

Xu H, Raynal N, Stathopoulos S, Myllyharju J, Farndale RW, Leitinger B, 2011 Collagen binding specificity of the discoidin domain receptors: binding sites on collagens II and III and molecular determinants for collagen IV recognition by DDR1. Matrix Biol 30, 16–26. [PubMed: 21044884]

Xu Y, Treumann S, Rossbacher R, Schneider S, Boor PJ, 2014 Dissecting aortic aneurysm induced by N-(2-aminoethyl) ethanolamine in rat: Role of defective collagen during development. Birth Defects Res A Clin Mol Teratol 100, 924–933. [PubMed: 24909928]

Xue M, Jackson CJ, 2015 Extracellular Matrix Reorganization During Wound Healing and Its Impact on Abnormal Scarring. Adv Wound Care (New Rochelle) 4, 119–136. [PubMed: 25785236]

Yamauchi M, Sricholpech M, 2012 Lysine post-translational modifications of collagen. Essays Biochem 52, 113–133. [PubMed: 22708567]

Yang Y, Yang Y, Trent MB, He N, Lick SD, Zimniak P, Awasthi YC, Boor PJ, 2004 Glutathione-S-transferase A4–4 modulates oxidative stress in endothelium: possible role in human atherosclerosis. Atherosclerosis 173, 211–221. [PubMed: 15064094]

Zgheib C, Xu J, Liechty KW, 2014 Targeting Inflammatory Cytokines and Extracellular Matrix Composition to Promote Wound Regeneration. Adv Wound Care (New Rochelle) 3, 344–355. [PubMed: 24757589]

Zhang Z, Finnerty CC, He J, Herndon DN, 2012 Smad ubiquitination regulatory factor 2 expression is enhanced in hypertrophic scar fibroblasts from burned children. Burns 38, 236–246. [PubMed: 21920670]

- Up to 90% of severely burned patients develop hypertrophic scarring.
- Most pharmacologic therapies are unsatisfactory.
- AEEA alters the structure of dermal extracellular matrix formed in vitro.
- Chemical structure–activity relationship of possible anti-fibrotic effects exists.
- Altering the hydroxyl or amino structure may increase AEEA's anti-fibrotic effects.

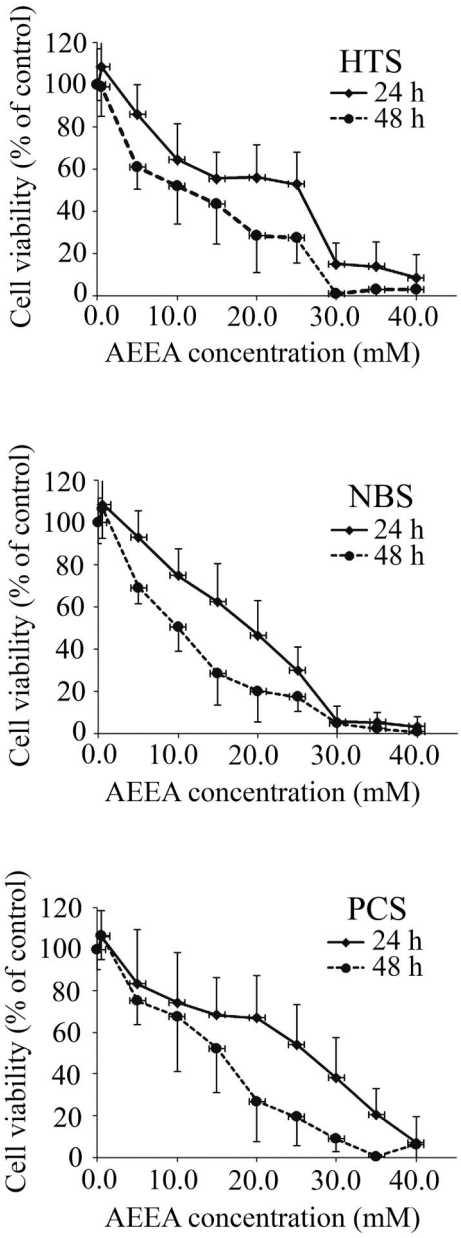

Figure 1. Cytotoxicity of AEEA in three human primary dermal fibroblast cell lines.

MTT assays were performed to determine cell viability. HTS, NBS or PCS cells were exposed to varying concentrations of AEEA (0.0, 0.5, 5.0, 10.0, 15.0, 20.0, 25.0, 30.0, 35.0, or 40.0 mM) for 24 h or 48 h. Absorbance values were read at 570 nm with a microplate reader, adjusted by subtracting the optical density of the media control, which is the media contained each corresponding concentration of AEEA in those wells without cells on the same plate, and normalized to the reading in the untreated control well. Four replicate wells were used for each assay. Values were the mean and SD of three separate experiments.

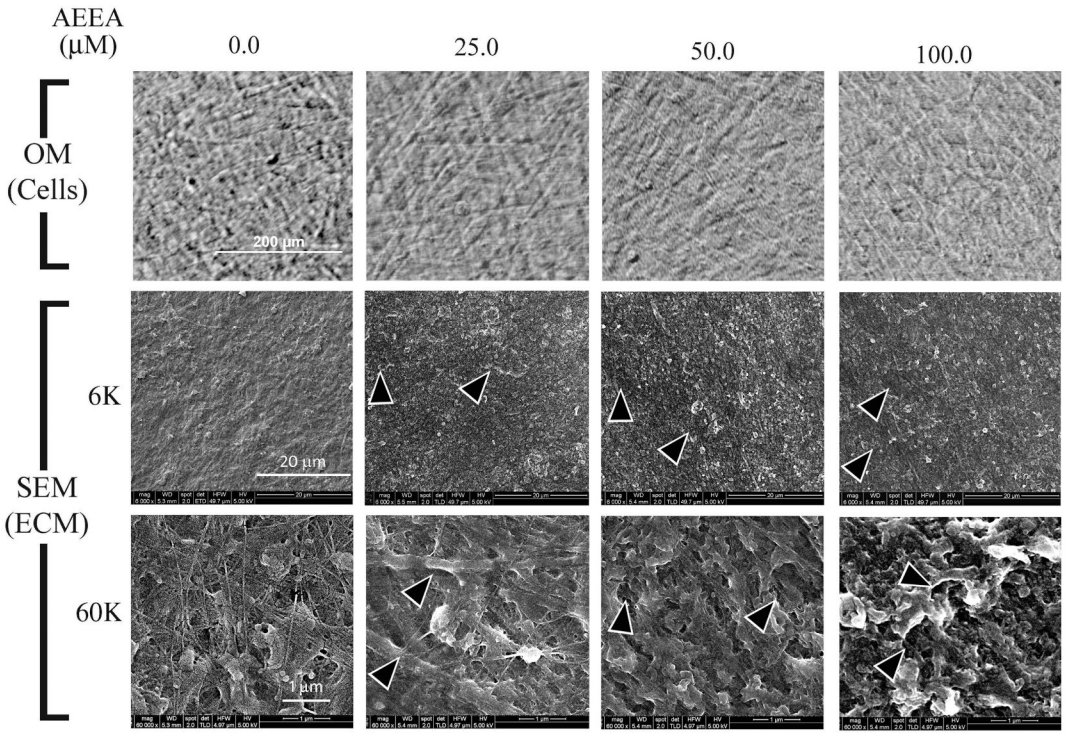

Figure 2. AEEA markedly altered the structure of the extracellular matrix produced *in vitro*.
Upper panel: Cells treated with AEEA (0.0, 25.0, 50.0, or 100 μM) for 14 days were observed under an optical microscope (OM) before decellularization. Middle and lower panels: ECM was examined with scanning electron microscopy (SEM) under low power (× 6,000 magnifications, middle panel) or high power (× 60,000 magnifications, lower panel). (See Results for detailed description).

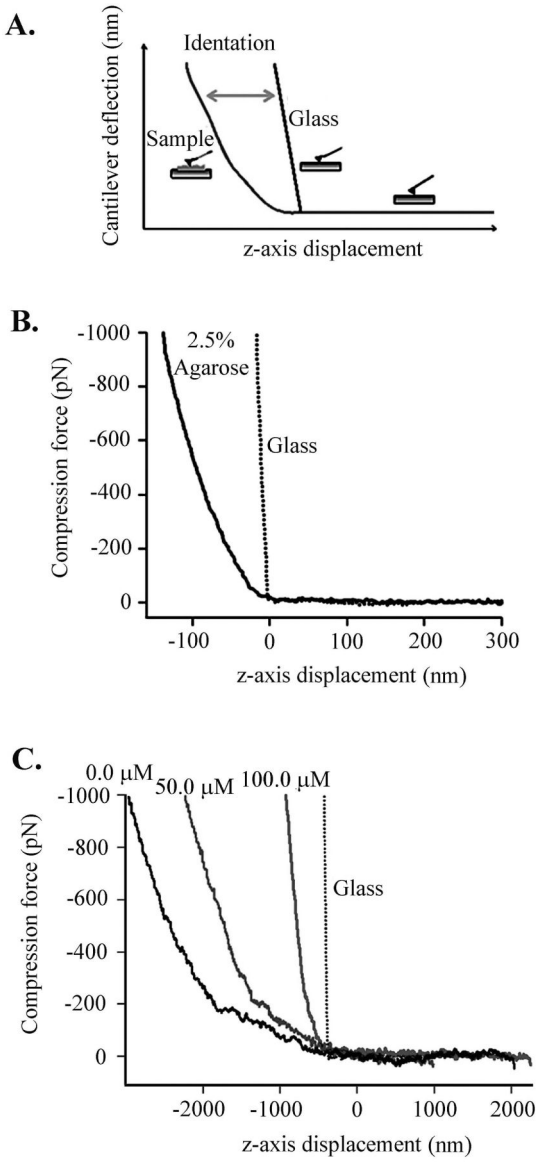

Figure 3. AFM compression analysis of ECM formed in vitro.

(A) Example of an AFM compression experiment. Elastic deformation is calculated by subtracting the force–displacement curve on glass, which served as a reference, from that on elastin film. (B) Force–displacement curves obtained on a glass coverslip and 2.5% agarose film. Agarose served as calibration reference, as it has a well-known elastic modulus of~ 0.02 MPa. The dotted line corresponds to the force-displacement curve on the glass coverslip. (C) Effect of AEEA (0.0, 50.0, or 100.0 μM) on force versus displacement during compression cycles. The average slope obtained for ECM samples with increasing concentrations of AEEA were as follows: 0.7 pN/nm (0.0 μM), 0.9 pN/nm (50.0 μM), and 3.1 pN/nm (100.0 μM).

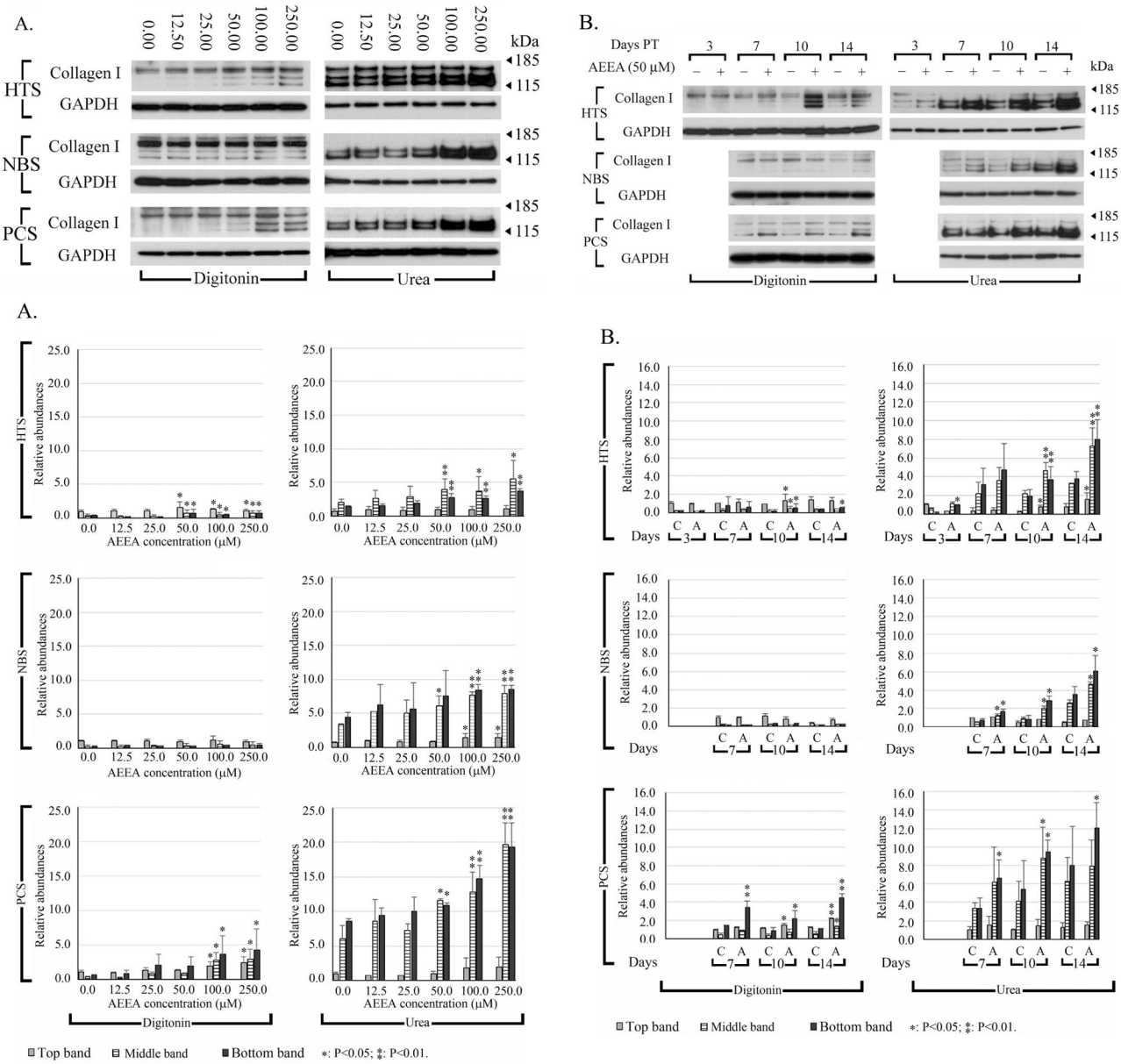

Figure 4. Effects of AEEA on extractability of type I collagen, and collagen deposition in three human fibroblast cell lines.

(A) Cells were treated with varying concentrations of AEEA for 10 days. (B) Time course of the effects of AEEA on the amount of extractable type I collagen protein. Cells were treated with 50 μM AEEA and harvested at the indicated time. Digitonin: samples extracted with native lysis buffer containing 1% digitonin. Urea: samples extracted with urea lysis buffer after native lysis buffer extraction. Densitometry analysis: relative abundances were normalized to the top band of the control sample of the digitonin fraction of each cell line, respectively. These results were representative of at least three independent biological replicates.

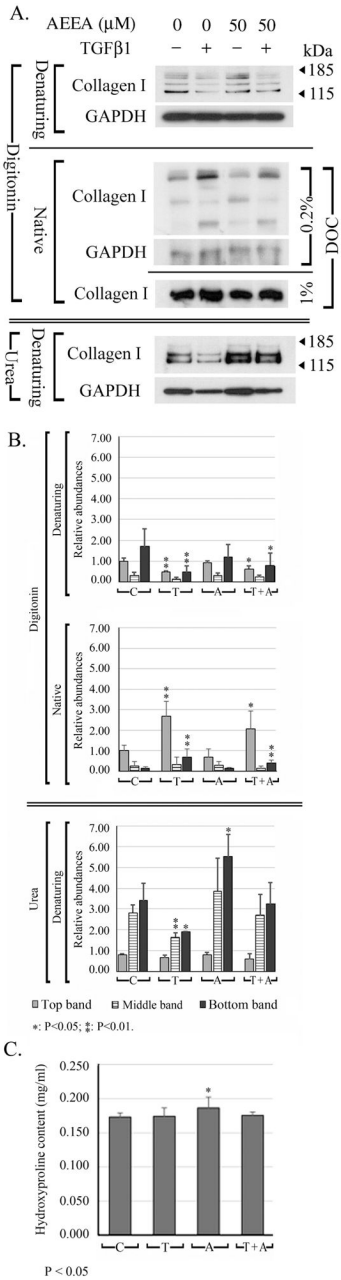

FIGURE 5. Effects of AEEA and TGF-β1 on extractability, electrophoretic behaviors of type I collagen, and collagen deposition.

A. Western blot analysis was performed on extracts under denaturing and native conditions to determine whether the extractability and the 3D structure of type I collagen may be altered by AEEA and TGF-β1. HTS fibroblasts were treated with AEEA (0 or 50 μM). 4 days after AEEA treatment, both AEEA and TGF-β1 (2.5 ng/ml) were added to the cells for 3 days, which were harvested later. DOC: sodium deoxycholate. B. Densitometry analysis: relative abundances were normalized to the top band of the control sample of the digitonin fraction. C. Quantitation of hydroxyproline in the pellets. (C: control; T: TGF-β1; A: AEEA;

T + A: TGF-β1 + AEEA). These results were representative of at least three independent biological replicates.

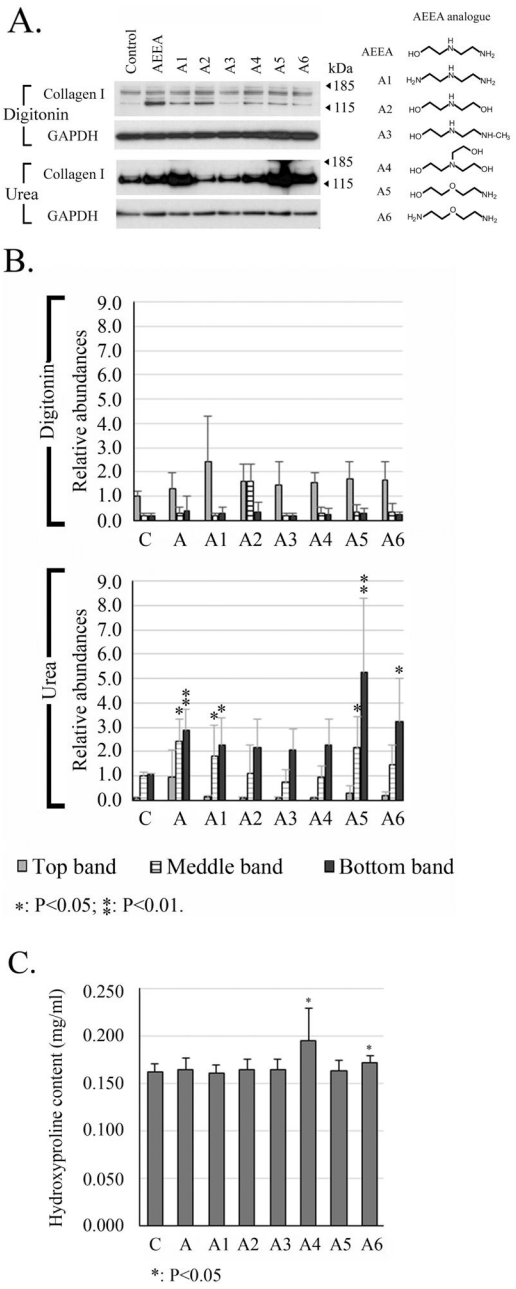

Figure 6. Chemical structure–activity relationship analysis of AEEA analogs.

HTS fibroblasts were treated with 50 μM of the indicated analog. A. The chemical structure of each is shown to the right. Western blots were performed to detect type I collagen. Digitonin: samples were extracted with native lysis buffer containing 1% digitonin. Urea: samples were extracted with urea lysis buffer after the extraction with native lysis buffer. B. Densitometry analysis: relative abundances were normalized to the top band of the control sample of the digitonin fraction. C. Quantitation of hydroxyproline in the pellets. (C: control; A: AEEA). These results were representative of at least three independent biological replicates.

Table 1.

LC_{50} for all three cell lines.

The median lethal concentration (LC_{50}), or the AEEA concentration producing 50% reduction in MTT absorbance, was determined by linear regression statistical analysis. Each corresponding linear regression equation and R-squared value is also shown. PT: post treatment.

Hours PT	Cells	LC_{50} (mM)	Regresion Equation	R-squared value
24	HTS	20.62	y = −0.0241x + 0.9969	R^2 = 0.9414
	NBS	19.14	y = −0.023 8x + 0.9848	R^2 = 0.9132
	PCS	23.48	y = −0.0222x + 1.0213	R^2 = 0.9657
48	HTS	14.75	y = −0.0246x + 0.8628	R^2 = 0.9085
	NBS	14.22	y = −0.0260x + 0.8697	R^2 = 0.8780
	PCS	16.70	y = −0.0267x + 0.9459	R^2 = 0.9363